THE JOURNAL OF PHYSICAL CHEMISTRY B

Article

pubs.acs.org/JPCB

Absorption of Carbon Dioxide, Nitrous Oxide, Ethane and Nitrogen by 1-Alkyl-3-methylimidazolium ($C_n$mim, n = 2,4,6) Tris(pentafluoroethyl)trifluorophosphate Ionic Liquids (eFAP)

D. Almantariotis, S. Stevanovic, O. Fandiño, A. S. Pensado, A. A. H. Padua, J.-Y. Coxam, and M. F. Costa Gomes*

Institut de Chimie de Clermont-Ferrand, Equipe Thermodynamique et Interactions Moléculaires, Clermont Université, Université Blaise Pascal, BP 80026, 63171 Aubiere, France

CNRS, UMR6296 ICCF, BP 80026, 63171 Aubiere, France

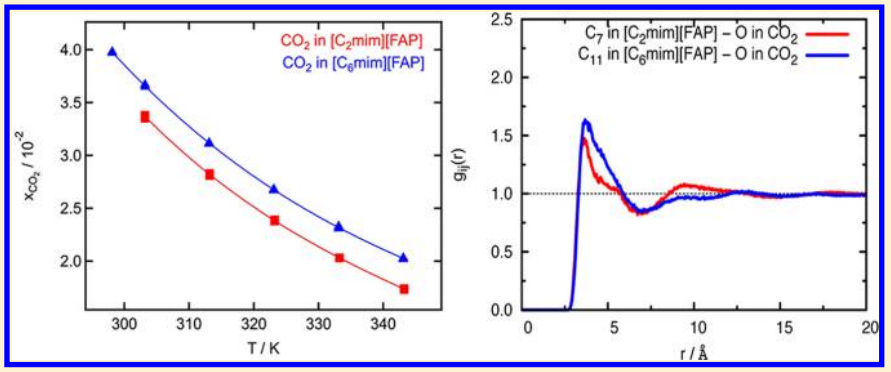

ABSTRACT: We measured the densities of 1-alkyl-3-methylimidazolium ($C_n$mim, n = 2,4,6) tris(pentafluoroethyl)-trifluorophosphate ionic liquids (eFAP) as a function of temperature and pressure and their viscosities as a function of temperature. These ionic liquids are less viscous than those based in the same cations but with other anions such as bis(trifluoromethylsulfonyl)imide. The ionic liquids studied are only partially miscible with water, their solubility increasing with the size of the alkyl side-chain of the cation and with temperature (from x_{H_2O} = 0.20 ± 0.03 for [C_4mim][eFAP] at 303.10 K to x_{H_2O} = 0.49 ± 0.07 for [C_6mim][eFAP] at 315.10 K). The solubility of carbon dioxide, nitrous oxide, ethane, and nitrogen in the three ionic liquids was measured as a function of temperature and at pressures close to atmospheric. Carbon dioxide and nitrous oxide are the more soluble gases with mole fraction solubilities of the order of 3×10^{-2} at 303 K. The solubility of these gases does not increase linearly with the size of the alkyl-side chain of the cation. The solubilities of ethane and nitrogen are much lower than those of carbon dioxide and nitrous oxide (mole fractions 60% and 90% lower, respectively). The higher solubility of CO_2 and N_2O can be explained by more favorable interactions between the solutes and the polar region of the ionic liquids as shown by the enthalpies of solvation determined experimentally and by the calculation of the site−site solute−solvent radial distribution functions using molecular simulation.

INTRODUCTION

Ionic liquids are considered promising media for gas separations[1] as they can selectively and efficiently absorb one gas in a mixture. In particular, they have been indicated as possible alternatives for carbon dioxide removal from flue-gas streams by chemical[2] or physical absorption.[3] Several properties are significant for the evaluation of ionic liquids as liquid absorbers for gaseous solutes—the absorption capacity, the selectivity, and the mass transfer—as they will determine the design and cost of possible industrial processes.[4]

We have studied the absorption of gases—carbon dioxide, nitrous oxide, ethane, and nitrogen—in ionic liquids based on the anion tris(pentafluoroethyl)trifluorophosphate and on a series of cations of the family of 1-alkyl-3-methylimidazolium ([$C_n$mim][eFAP] with n = 2,4,6). This new class of ionic liquids containing fluorinated anions was first synthesized by Ignat'ev et al.[5] as replacements for ionic liquids containing other fluorous groups in the anion, namely, hexafluorophosphate, that might be hydrolytically unstable, especially at elevated temperature.

Other authors have previously studied gas absorption in eFAP-based ionic liquids. Both Muldoon et al.[6] and Yokozeki et al.[7] have measured the absorption of carbon dioxide in [C_6mim]-[eFAP] at temperatures from 298 to 333 K and at pressures up to 15 MPa and at 298 K and up to 2 MPa, respectively. Blath et al.[8] also studied the carbon dioxide absorption in the same ionic liquid and have compared it with that of nitrogen at 333.15 K.

Received: May 9, 2012
Revised: June 7, 2012
Published: June 8, 2012

ACS Publications © 2012 American Chemical Society

dx.doi.org/10.1021/jp304501p | J. Phys. Chem. B 2012, 116, 7728−7738

Different predictive models have been used to assess gas absorption in these ionic liquids. Zhang et al.[9] have used COSMO-RS to predict the solubility of carbon dioxide in [C_6mim][eFAP] at 298 K, the values obtained being compared with experimental data obtained by the same authors at temperatures from 283 to 323 K. Finally, Zhang et al.[10] have used Monte Carlo simulation methods to study the same system between 298 and 323 K and at pressures of gas from 0.25 to 2.0 MPa.

This work is the continuation of a previous effort to explain the influence of fluoro-moieties in ionic liquids on the gas absorption by ionic liquids.[11] After concluding that the presence of fluorinated alkyl-side chains in imidazolium cations significantly influenced the absorption of carbon dioxide, we have decided to study the effect of the fluorination in the anion. We expect to clarify the mechanisms of gas solvation in these media by associating experimental determinations of the solubility of apolar gases such as nitrogen and ethane, a quadrupolar gas such as carbon dioxide, and a polar gas as nitrous oxide with molecular simulations, capable of providing insights into the structure of the solutions. The present study will also contribute to the choice of promising liquid absorbents for gases having an important environmental impact such as carbon dioxide and nitrous oxide by evaluating both the absorption capacity and the selectivity of different ionic liquids.

EXPERIMENTAL SECTION

Materials. The samples of ionic liquids used were purchased from Merck with mole fraction purities of 0.995. Their decomposition temperatures were determined using a modulated DSC 2920 from TA Instruments and were found to be 580 and 583 K for [C_4mim][eFAP] and [C_6mim][eFAP], respectively.

The ionic liquids were kept under vacuum for 15 h at 303 K before each measurement. The water contents of each degassed sample were determined, with a precision of ±5 ppm, using a coulometric Karl Fisher titrator (Mettler Toledo DL32). The water content of the degassed samples was found be 7 ppm for [C_2mim][eFAP], 11 ppm for [C_4mim][eFAP], and 23 ppm for [C_6mim][eFAP].

The gases were used as received from the manufacturer. Carbon dioxide was obtained from AGA/Linde Gas with a mole fraction purity of 0.99995; nitrous oxide was obtained from Linde with a mole fraction purity of 0.995; ethane was purchased at AGA/Linde GAZ with a mole fraction purity of 0.995, and nitrogen was obtained from SAGA with a mole fraction purity of 0.998.

Density Measurements. Densities were measured using a U-shape vibrating-tube densimeter (Anton Paar, model DMA 512) operating in a static mode, following the procedure described in previous publications.[12,13] Measurements for [C_2mim][eFAP], [C_4mim][eFAP], and [C_6mim][eFAP] were performed for pressures up to 25 MPa and at temperatures from 293 to 353 K.

The temperature in the densimeter was maintained constant to within ±0.01 K by means of a recirculating bath equipped with a PID temperature controller (Julabo FP40-HP). For measuring the temperature, a 100 Ohm platinum resistance thermometer (precision of ±0.02 K and accuracy of ±0.04 K) was used. Its calibration was performed by verifying a water triple point (triple point cell by Hart Scientific) and by comparison against a 100 Ohm platinum resistance Hart Scientific model 1502A. The pressure was measured using a precision pressure transmitter Druck, model PTX 610, working in a range from 0 to 70 MPa with an uncertainty of 0.08% full scale.

The measured period of vibration (τ) of a U tube is related to the density (ρ) according to: $\rho = A\tau^2 + B$, where A and B are parameters that are function of temperature and pressure determined by calibration between temperatures of 293 and 343 K (and pressures of 0.1 and 25 MPa), using as calibration fluids *n*-heptane, bromobenzene and 2,4-dichlorotoluene following the recommendations by Schilling et al.[14] Density measurements were performed in steps of 10 K. The uncertainty of the density measurements is estimated as 10^{-4} g cm^{-3}.

Viscosity Measurements. The dynamic viscosities of the three ionic liquids [C_2mim][eFAP], [C_4mim][eFAP], and [C_6mim][eFAP], previously dried under vacuum, were measured using an Anton Paar AMVn rolling ball viscosimeter, as a function of the temperature from 293.15 to 373.15 K (controlled to within 0.01 K and measured with an accuracy better than 0.05 K) and at atmospheric pressure. Before starting the measurements, the 3 mm diameter capillary tube was calibrated as a function of temperature and angle of measurement using a standard viscosity oil from Cannon (N35). The overall uncertainty on the viscosity is estimated as ±1.5%.

Gas-Solubility Measurements. The experimental method used for the gas solubility measurements is based on an isochoric saturation technique and has been described in previous publications.[15,16] In this technique, a known quantity of gaseous solute is put in contact with a precisely determined quantity of degassed solvent at a constant temperature inside an accurately known volume. When thermodynamic equilibrium is attained, the pressure above the liquid solution is constant and is directly related to the solubility of the gas in the liquid.

The quantity of ionic liquid introduced in the equilibration cell is determined gravimetrically. This quantity is equal to the amount of solvent present in the liquid solution, n_1^{liq}, as the ionic liquid does not present a measurable vapor pressure. The amount of solute present in the liquid solution, n_2^{liq} (subscripts 1 and 2 stand for solvent and solute, respectively), is calculated by the difference between two *pVT* measurements: first when the gas is introduced in a calibrated bulb with volume V_{GB}, and second after thermodynamic equilibrium is reached:

$$n_2^{liq} = \frac{p_{ini} V_{GB}}{[Z_2(p_{ini}, T_{ini})RT_{ini}]} - \frac{p_{eq}(V_{tot} - V_{liq})}{[Z_2(p_{eq}, T_{eq})RT_{eq}]} \quad (1)$$

where p_{ini} and T_{ini} are the pressure and temperature in the first *pVT* determination and p_{eq} and T_{eq} are the pressure and temperature at the equilibrium. V_{tot} is the total volume of the equilibration cell, V_{liq} is the volume of the liquid solution, and Z_2 is the compression factor for the pure gas. The solubility can then be expressed in mole fraction, or as Henry's law constant:

$$K_H = \lim_{x_2 \to 0} \frac{f_2(p, T, x_2)}{x_2} \cong \frac{\phi_2(p_{eq}, T_{eq})p_{eq}}{x_2} \quad (2)$$

where f_2 is the fugacity of the solute and ϕ_2 its fugacity coefficient.

We consider that the volume of the ionic liquid does not change when the gas is solubilized, and so the volume of the liquid solution is equal to the molar volume of the pure ionic liquid.

Water-Miscibility Measurements. The miscibility gap of [C_4mim][eFAP] with water and [C_6mim][eFAP] with water was determined at different temperatures using a *pVT* method that has been described in a previous publication.[17] An equilibrium cell equipped with precision manometers and placed in an air thermostat was used. Precisely known quantities of ionic liquid

dx.doi.org/10.1021/jp304501p | J. Phys. Chem. B 2012, 116, 7728−7738

Table 1. Experimental Densities, ρ, of the Ionic Liquids [C_2mim][eFAP], [C_6mim][eFAP], and [C_4mim][eFAP] between 293 and 353 K and up to 25 MPa

T/K	$p/10^5$ Pa	ρ/(kg·m^{-3})	T/K	$p/10^5$ Pa	ρ/(kg·m^{-3})
		[C_2mim][eFAP]			
293.14	1.01	1713.4	323.16	1.01	1677.5
293.13	5.00	1713.7	323.14	5.00	1678.1
293.13	10.0	1714.2	323.13	10.0	1678.6
293.14	25.0	1715.4	323.15	25.0	1680.1
293.14	50.0	1717.7	323.14	50.0	1682.6
293.14	100	1722.0	323.13	100	1687.4
293.13	150	1726.3	323.14	150	1692.1
293.13	200	1730.4	323.13	200	1696.7
293.13	250	1734.5	323.13	250	1701.1
303.16	1.01	1701.3	333.18	1.01	1665.6
303.17	5.00	1701.7	333.17	5.00	1666.2
303.18	10.0	1702.2	333.18	10.0	1666.7
303.18	25.0	1703.4	333.18	25.0	1668.2
303.19	50.0	1705.7	333.18	50.0	1670.8
303.22	100	1710.2	333.18	100	1675.8
303.19	150	1714.7	333.19	150	1680.7
303.18	200	1719.0	333.17	200	1685.5
303.19	250	1723.1	333.18	250	1690.0
313.15	1.01	1689.4	343.18	1.01	1653.9
313.17	5.00	1689.8	343.13	5.00	1654.7
313.18	10.0	1690.3	343.14	10.0	1655.2
313.18	25.0	1691.7	343.16	25.0	1656.8
313.17	50.0	1694.1	343.13	50.0	1659.5
313.18	100	1698.7	343.14	100	1664.7
313.17	150	1703.3	343.13	150	1669.8
313.16	200	1707.7	343.13	200	1674.6
313.17	250	1712.0	343.13	250	1679.4
		[C_6mim][eFAP]			
293.16	1.03	1556.1	323.17	1.03	1523.1
293.17	2.53	1556.3	323.16	2.53	1523.2
293.16	5.00	1556.6	323.14	5.00	1523.5
293.17	10.0	1557.0	323.15	10.0	1524.1
293.18	25.0	1558.1	323.15	25.0	1525.6
293.16	50.0	1560.6	323.19	50.0	1528.0
293.16	100	1564.8	323.19	100	1532.8
293.16	150	1569.0	323.19	150	1537.4
293.16	200	1573.1	323.19	200	1541.9
293.16	250	1577.0	323.19	250	1546.2
303.18	1.03	1544.9	333.19	1.03	1512.6
303.18	2.53	1545.1	333.19	2.53	1512.8
303.17	5.00	1545.3	333.19	5.00	1513.0
303.18	10.0	1545.8	333.19	10.0	1513.5
303.18	25.0	1547.2	333.19	25.0	1515.1
303.18	50.0	1549.5	333.19	50.0	1517.7
303.18	100	1554.0	333.19	100	1522.6
303.18	150	1558.3	333.19	150	1527.4
303.18	200	1562.5	333.19	200	1532.1
303.19	250	1566.5	333.18	250	1536.6
313.17	1.03	1534.1	343.19	1.03	1502.0
313.18	2.53	1534.2	343.18	2.53	1502.2
313.19	5.00	1534.4	343.18	5.00	1502.4
313.19	10.0	1535.0	343.18	10.0	1503.0
313.19	25.0	1536.4	343.18	25.0	1504.7
313.19	50.0	1538.8	343.16	50.0	1507.4
313.19	100	1543.3	343.15	100	1512.6
313.19	150	1547.8	343.14	150	1517.6
313.19	200	1552.2	343.13	200	1522.4
313.18	250	1556.4	343.13	250	1527.0
		[C_4mim][eFAP]			
293.18	1.05	1629.1	333.14	1.01	1584.0
293.18	5.00	1639.4	333.11	4.99	1584.4
293.18	10.0	1629.9	333.08	10.0	1585.0
293.18	25.0	1631.2	333.08	25.0	1586.6
293.18	50.0	1633.5	333.05	50.0	1589.3
293.18	100	1637.9	333.04	100	1594.3
293.18	150	1642.2	333.04	150	1599.2
293.18	200	1646.3	333.03	200	1603.9
293.18	250	1650.3	333.02	250	1608.5
303.21	1.02	1617.6	343.14	1.01	1573.1
303.22	4.98	1618.0	343.14	4.99	1573.5
303.23	10.0	1618.5	343.14	10.0	1574.1
303.26	25.0	1619.8	343.14	25.0	1575.8
303.26	50.0	1622.1	343.13	50.0	1578.5
303.26	100	1626.7	343.13	100	1583.7
303.26	150	1631.1	343.14	150	1588.8
303.27	200	1635.4	343.14	200	1593.7
303.28	250	1639.5	343.14	250	1598.4
313.15	1.01	1606.4	353.05	1.00	1562.5
313.14	5.00	1606.8	353.04	5.00	1562.9
313.16	10.0	1607.3	353.05	10.0	1563.5
313.18	25.0	1608.7	353.04	25.0	1565.3
313.18	50.0	1611.2	353.04	50.0	1568.1
313.18	100	1615.9	353.03	100	1573.5
313.18	150	1620.4	353.03	150	1578.7
313.19	200	1624.8	353.02	200	1583.8
313.20	250	1629.1	353.02	250	1588.6
323.19	1.01	1594.9			
323.21	5.00	1595.3			
323.21	10.0	1595.8			
323.20	25.0	1597.4			
323.20	50.0	1599.9			
323.20	100	1604.8			
323.20	150	1609.5			
323.22	200	1614.1			
323.23	250	1618.4			

and water, previously degassed under vacuum and by successive melting and freezing cycles, respectively, are put in contact, under their own vapor pressure, inside the equilibrium cell. The two components are mixed at constant temperature and in the constant and accurately known volumes of the apparatus. When thermodynamic equilibrium is reached, the vapor pressure is recorded. The composition of the liquid mixture is modified by evacuating the molecular compound, the new composition of the mixture being calculated gravimetrically. The temperature of the equilibrium cell and of the manometer was controlled to

Table 2. Tait Parameters C, B_0, B_1, and B_2 Used to Smooth the Experimental Densities as a Function of Pressure (to 25 MPa) and Temperature (from 293 to 353K) along with the Standard Deviation of the Fit, s

ionic liquid	$10^2 \cdot C$	B_0/ MPa	B_1/ MPa·K^{-1}	$10^3 \cdot B_2$/ MPa·K^{-2}	s
[C_2mim][eFAP]	+7.713	+413.748	−1.182	+0.912	0.01
[C_4mim][eFAP]	+6.922	+325.658	−0.871	+0.597	0.01
[C_6mim][eFAP]	+6.997	+289.715	−0.655	+0.253	0.01

dx.doi.org/10.1021/jp304501p | J. Phys. Chem. B 2012, 116, 7728−7738

Table 3. Experimental Dynamic Viscosities, η, of the Ionic Liquids [C_2mim][eFAP], [C_4mim][eFAP], and [C_6mim][eFAP] as a Function of Temperature at Atmospheric Pressure

	η/mPa s		
T/K	[C_2mim][eFAP]	[C_4mim][eFAP]	[C_6mim][eFAP]
293.15	74.71	100.3	118.8
303.15	48.34	62.36	70.75
313.15	33.36	42.04	45.57
323.15	24.38	29.24	31.64
333.15	18.10	20.84	22.15
343.15	14.01	15.50	16.38
353.15	11.18	11.88	12.49
363.15	9.041	9.337	9.754
373.15	7.447	7.527	7.878

Table 4. Experimental values of the vapour pressures $p_{mix}^{H_2O}$ of the [C_4mim][eFAP] + water and [C_6mim][eFAP] + water mixtures as a function of the composition, expressed in water mole fraction, x_{H_2O}

[C_4mim][eFAP] + H_2O T = 303.08 K		[C_6mim][eFAP] + H_2O T = 303.40 K		[C_6mim][eFAP] + H_2O T = 315.10 K	
x_{H_2O}	$p_{mix}^{H_2O}/10^2$ Pa	x_{H_2O}	$p_{mix}^{H_2O}/10^2$ Pa	x_{H_2O}	$p_{mix}^{H_2O}/10^2$ Pa
0.0519	15	0.072	18	0.068	16
0.0782	21	0.083	14	0.077	20
0.0817	23	0.098	18	0.103	33
0.0839	21	0.101	9	0.134	44
0.1050	23	0.161	20	0.139	39
0.2090	32	0.260	29	0.430	68
0.2830	38	0.386	36	0.564	75
0.4123	39	0.486	38	0.631	77
0.4797	39	0.530	39	0.668	77
0.4925	39	0.571	39	0.734	76
0.4935	39	0.611	39	0.777	77
0.5514	38	0.698	40	0.781	77
0.5874	39	0.715	40	0.820	77
0.6102	39	0.733	40	0.843	77
0.6615	39	0.751	40	0.853	77
0.7090	39	0.789	40	0.878	80
0.8299	39	0.815	40	0.883	77
		0.827	40	0.926	77
		0.832	41		
		0.840	40		
		0.858	40		
		0.875	41		
		0.881	40		
		0.884	40		
		0.898	40		
		0.899	40		
		0.914	41		

within ±0.01 K, in the temperature range of 288 to 313 K, and measured with a calibrated 100 Ohm platinum resistance thermometer from Hart Scientific (Secondary Reference Temperature Standard, model 1502A, accuracy of ±0.018 at 273 K). The pressure was measured using a quartz spiral manometer from Ruska (model 2465, uncertainty ±10^{-5} bar) for [C_4mim][eFAP] and a precision manometer from Druck DPI 262 (3.5−140 kPa, uncertainty ±0.1% full scale) for [C_6mim][eFAP].

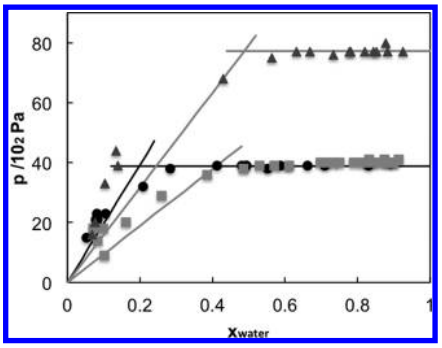

Figure 1. Vapor pressures of the [C_4mim][eFAP] + water and [C_6mim][eFAP] + water mixtures as a function of the composition: ●, [C_4mim][eFAP] + water at 303.10 K; ■, [C_6mim][eFAP] + water at 303.40 K; ▲, [C_6mim][eFAP] + water at 315.10 K.

Table 5. Experimental Values of Gases (CO_2, N_2O) in [C_2mim][eFAP] Expressed Both as Henry's Law Constants, K_H and as CO_2 Mole Fraction, x_2, Corrected for a Partial Pressure of Solute of 0.1 MPa[a]

T /K	p /10^2 Pa	K_H /10^5 Pa	x_2 /10^{-2}	dev %
		CO_2		
303.18	643.97	29.7	3.35	+ 0.6
303.18	536.22	29.4	3.38	− 0.4
303.18	625.41	29.4	3.38	− 0.4
313.16	672.57	35.5	2.81	+ 0.6
313.17	559.80	35.2	2.83	− 0.2
323.18	700.35	41.9	2.38	+ 0.2
323.21	679.96	41.8	2.38	− 0.1
323.22	582.84	41.7	2.39	− 0.3
333.20	727.51	49.2	2.03	+ 0.1
333.24	605.37	49.1	2.03	− 0.2
343.18	753.91	57.1	1.74	− 0.4
343.20	731.78	57.4	1.74	+ 0.1
343.23	627.50	57.6	1.73	+ 0.4
		N_2O		
303.15	546.68	28.7	3.47	− 0.1
303.16	496.96	28.9	3.45	+ 0.6
303.19	529.59	28.5	3.49	− 0.8
313.16	571.19	34.3	2.91	+ 0.2
313.17	518.65	34.6	2.87	+ 1.1
313.19	552.82	34.0	2.93	− 0.7
323.16	594.95	40.5	2.46	− 0.6
323.16	539.72	41.2	2.42	+ 1.2
323.19	575.66	40.5	2.46	− 0.6
333.14	618.11	47.6	2.09	− 1.5
333.20	560.49	48.8	2.04	+ 0.9
343.13	641.14	56.1	1.78	− 1.9
343.14	620.82	58.5	1.70	+ 2.2
343.23	580.80	57.3	1.74	+ 0.0

[a] p is the experimental equilibrium pressure and the percent deviation is relative to the correlations of the data reported in Table 8.

Molecular Simulation. The ionic liquids [C_2mim][eFAP] and [C_6mim][eFAP] were represented by an all-atom force field[18−20] based on the OPLS_AA framework[21,22] but developed specifically for ionic liquids. The force-field model contains the parameters required to simulate the [eFAP]$^-$ anion and the 1-alkyl-3-methylimidazolium cations. The functional form of the force field contains four kinds of potential energy: stretching of covalent bonds, bending of valence angles, torsion around dihedral angles, and nonbonded interactions. Nonbonded interactions are

dx.doi.org/10.1021/jp304501p | J. Phys. Chem. B 2012, 116, 7728−7738

Table 6. Experimental Values of Gases (CO_2, N_2O, C_2H_6, and N_2) in [C_4mim][eFAP] Expressed Both as Henry's Law Constants, K_H and as CO_2 Mole Fraction, x_2, Corrected for a Partial Pressure of Solute of 0.1 MPa[a]

T /K	p /10^2 Pa	K_H /10^5 Pa	x_2 /10^{-2}	dev %
		CO_2		
303.16	658.5	25.0	3.99	+ 0.1
303.16	655.1	25.0	3.98	+ 0.2
303.18	665.0	24.8	4.01	− 0.4
313.15	686.0	29.3	3.40	+ 0.1
313.17	691.7	29.3	3.40	− 0.1
313.18	684.3	29.4	3.39	+ 0.2
323.20	717.9	34.1	2.92	+ 0.0
323.20	712.9	34.0	2.93	− 0.1
323.23	712.5	34.1	2.93	+ 0.0
333.21	743.6	39.3	2.53	+ 0.5
333.23	739.2	39.1	2.55	− 0.3
333.24	739.9	39.0	2.55	− 0.3
343.24	766.8	44.4	2.24	− 0.5
343.24	764.9	44.4	2.24	− 0.5
343.27	769.1	45.1	2.21	+ 1.1
		N_2O		
303.15	651.0	23.7	4.20	+ 0.1
303.16	851.7	23.6	4.21	− 0.2
303.17	860.0	23.8	4.19	+ 0.3
313.16	886.1	27.7	3.59	+ 1.6
313.17	675.4	26.4	3.77	− 3.3
313.18	894.6	27.7	3.60	+ 1.4
323.16	919.4	32.0	3.11	+ 2.9
323.17	701.0	30.4	3.27	− 2.3
323.19	926.6	30.8	3.24	− 1.2
333.15	952.1	36.6	2.73	+ 3.6
333.17	726.1	34.7	2.87	− 1.7
333.20	959.6	34.9	2.86	− 1.1
343.06	983.8	41.2	2.42	+ 3.9
343.17	750.3	38.6	2.58	− 2.7
343.21	991.9	39.0	2.56	− 1.7
		C_2H_6		
303.26	943.7	57.5	1.73	− 1.4
303.56	946.4	58.6	1.69	+ 0.2
303.57	954.9	59.2	1.68	+ 1.2
313.24	977.5	66.7	1.49	+ 0.5
313.25	975.6	65.7	1.51	− 1.0
313.27	986.5	66.6	1.49	+ 0.4
323.21	1009.4	76.2	1.31	+ 1.3
323.22	1007.3	75.0	1.33	− 0.2
323.28	1018.9	74.6	1.33	− 0.8
333.16	1041.1	85.6	1.16	+ 0.8
333.17	1050.8	83.4	1.19	− 1.7
333.32	1039.4	85.5	1.16	+ 0.6
343.15	1083.0	93.1	1.07	− 2.5
343.15	1072.8	95.9	1.04	+ 0.6
343.33	1071.1	97.5	1.02	+ 1.9
		N_2		
303.17	910.4	241.9	0.413	+ 2.4
303.17	911.1	236.3	0.423	+ 0.1
303.17	911.05	234.7	0.426	− 0.6
303.18	915.9	231.6	0.432	− 1.9
313.16	940.8	247.9	0.403	+ 0.5
313.18	940.1	252.6	0.396	+ 2.3
313.19	940.75	246.2	0.406	− 0.2
313.19	945.7	240.1	0.417	− 2.8
323.15	970.3	257.1	0.389	− 0.3
323.19	975.6	254.4	0.393	− 1.4
323.20	969.7	262.5	0.381	+ 1.7
323.20	970.4	257.4	0.389	− 0.3
333.14	999.8	266.3	0.376	− 1.4
333.20	1000	269.2	0.372	− 0.3
333.20	999.4	279.3	0.358	+ 3.4
333.20	1005.4	266.5	0.375	− 1.3
343.13	1028.8	297.2	0.337	+ 5.0
343.16	1029.4	279.3	0.358	− 1.1
343.20	1029.5	278.0	0.360	− 1.6
343.22	1035.2	275.0	0.364	− 2.7

[a] p is the experimental equilibrium pressure, and the percent deviation is relative to the correlations of the data reported in Table 8.

active between atoms of the same molecule separated by more than three bonds and between atoms of different molecules. The potential energy associated with bonds and angles is described by harmonic terms, dihedral torsion energy is represented by a series of cosines, and nonbonded interactions are given by the Lennard-Jones sites and by Coulomb interactions (calculated using the Ewald summation method) between partial point charges placed on the atomic sites. The two ionic liquids considered were simulated in periodic cubic boxes containing 400 and 320 ion pairs for [C_2mim][eFAP] and [C_6mim][eFAP], respectively, using the molecular dynamics method implemented in the DL_POLY package.[23] The initial configurations were lattices with low density. Equilibrations starting from the low density arrangement of ions took 2 ns, at constant NpT and T = 423 K, with a time step of 2 fs (covalent bonds involving H atoms were considered rigid constraints). Once the equilibrium density was attained, simulation runs of 1 ns were performed. At the final densities of the ionic liquid state, the length of the side of the simulation boxes is approximately 60 Å for both ionic liquids. Additionally, simulation boxes containing 400 ion pairs of [C_2mim][eFAP] and eight CO_2 or N_2O molecules, and 320 ion pairs of [C_6mim][eFAP] and eight molecules of gas were prepared, to calculate solute−solvent radial distribution functions (RDFs) between the gas and the ionic liquid. We consider this reduced number of solute molecules in order to minimize solute−solute interactions, but still yielding good sampling of the liquid phase structure. The potential model of Harris and Yung[24] was used for CO_2, whereas the parameters for N_2O were those proposed by Costa Gomes et al.[25]

The chemical potentials of CO_2 and N_2O at 373 K in the two ionic liquids were calculated in a two-step procedure, similar to that used in previous works.[11,26] First, for both CO_2 and N_2O, a reduced-size version of the molecule was produced by subtracting 0.8 Å from the C−O, N−N, and N−O bond length and also from the Lennard-Jones diameters σ_O, σ_C (CO_2), and σ_N, σ_O (N_2O). The resulting molecules are small enough so that their chemical potentials can be calculated using the Widom test-particle insertion method[27] with efficient statistics.[26] For this calculation, we performed simulation runs of 600 ps at 373 K, from which 3000 configurations were stored. Then, 10^5 insertions were attempted in each of the 3000 stored configurations of the pure ionic liquids. Second, a stepwise finite-difference thermodynamic integration procedure[28] was used to calculate the free-energy difference between the initial, reduced versions of the

dx.doi.org/10.1021/jp304501p | J. Phys. Chem. B 2012, 116, 7728−7738

Table 7. Experimental Values of Gases (CO_2, N_2O, and C_2H_6) in [C_6mim][eFAP] Expressed Both as Henry's Law Constants, K_H, and as CO_2 Mole Fraction, x_2, Corrected for a Partial Pressure of Solute of 0.1 MPa[a]

T /K	p /10^2 Pa	K_H /10^5 Pa	x_2 /10^{-3}	dev %
		CO_2		
298.13	613.0	25.1	3.97	− 0.2
298.13	587.4	25.1	3.98	− 0.1
303.18	601.6	27.2	3.67	+ 0.4
303.22	627.2	27.3	3.65	+ 0.1
313.10	629.5	32.0	3.12	+ 0.1
313.10	654.6	32.1	3.11	− 0.3
323.07	681.2	37.3	2.67	− 0.2
323.08	656.7	37.3	2.68	+ 0.1
333.05	707.4	43.1	2.31	− 0.3
333.08	683.0	42.9	2.33	+ 0.3
343.06	733.0	49.3	2.02	− 0.1
343.08	709.1	49.2	2.03	+ 0.1
		N_2O		
303.16	500.4	23.4	4.26	+ 0.8
303.18	589.4	23.8	4.18	− 0.9
303.18	532.8	23.6	4.23	+ 0.3
313.15	557.2	28.1	3.55	+ 0.1
313.15	522.5	28.0	3.56	+ 0.5
313.18	615.2	28.4	3.51	− 0.9
323.15	580.8	33.2	3.00	+ 0.2
323.15	544.0	33.1	3.01	+ 0.5
323.21	640.5	33.6	2.97	− 0.8
333.13	565.1	39.1	2.54	+ 0.3
333.16	603.8	39.0	2.56	+ 0.6
333.24	665.1	39.4	2.53	− 0.5
343.16	585.9	45.9	2.17	− 0.2
343.17	626.4	45.4	2.20	+ 1.0
343.26	689.3	46.3	2.15	− 0.9
		C_2H_6		
303.14	520.4	59.8	1.67	+ 0.6
303.14	580.6	60.2	1.65	− 0.1
303.15	528.7	60.8	1.64	− 1.1
313.12	539.3	68.5	1.45	+ 1.0
313.12	547.6	69.0	1.45	+ 0.3
323.12	558.4	79.1	1.26	+ 1.4
323.12	623.2	80.9	0.911	− 0.9
323.13	567.1	81.1	1.23	− 1.1
333.12	577.6	93.3	1.07	+ 0.3
333.16	586.4	94.4	1.06	− 0.8
343.12	596.6	109	0.917	+ 0.7
343.13	665.6	110	0.911	+ 0.1
343.14	605.5	110	0.907	− 0.3

[a] p is the experimental equilibrium pressure, and the percent deviation is relative to the correlations of the data reported in Table 8.

carbon dioxide and nitrous oxide molecules and the full-size model. The free-energy calculation was performed over 10 intermediate steps along a linear path connecting the intermolecular parameters (bonds and diameters) of the reduced-size molecules to those of the full-size molecules. We selected this number of intermediate steps because the starting point and the final state of the thermodynamic integration route are not too far. A large number of intermediate steps would be required if we intended to calculate the chemical potential of CO_2 or N_2O by thermodynamic integration starting from the pure solvent. In the finite-difference thermodynamic integration scheme, derivatives (finite differences) of the total energy of the system with respect

Table 8. Parameters of Eq 11 Used to Smooth the Experimental Results on K_H from Tables 5− 7 along with the Percent Standard Deviation of the Fit (s)

gas	A_0	A_1	A_2	s
		[C_2mim][eFAP]		
CO_2	+ 10.14	− 2.413 × 10^3	+ 1.104 × 10^5	0.4
N_2O	+ 13.66	− 4.631 × 10^3	+ 4.568 × 10^5	1.1
		[C_4mim][eFAP]		
CO_2	+ 7.649	− 1.253 × 10^3	− 5.784 × 10^4	0.4
N_2O	+ 7.623	− 1.366 × 10^3	+ 4.288 × 10^3	2.3
C_2H_6	+ 10.07	− 2.429 × 10^3	+ 1.842 × 10^5	1.2
N_2	+ 8.597	− 1.497 × 10^3	+ 1.659 × 10^5	2.0
		[C_6mim][eFAP]		
CO_2	+ 8.703	− 1.744 × 10^3	+ 3.286 × 10^4	0.2
N_2O	+ 11.06	− 3.154 × 10^3	+ 2.298 × 10^5	0.7
C_2H_6	+ 17.22	− 6.719 × 10^3	+ 8.306 × 10^5	0.7

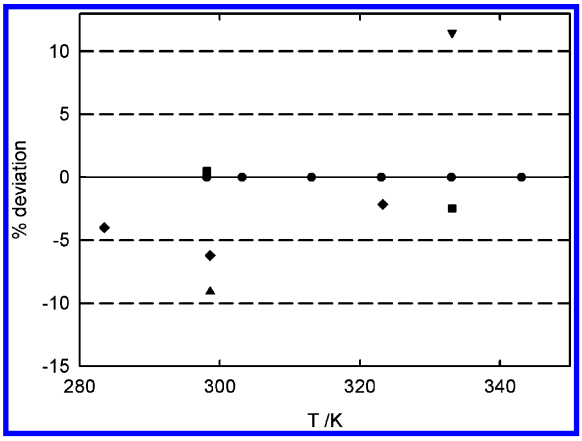

Figure 2. Percent deviations from the literature values to the correlation of the Henry's law constants obtained in this work for carbon dioxide in [C_6mim][eFAP]: (●) this work; (■) Muldoon et al.; (▲) Yokozeki et al.; (♦) Zhang et al.; (▼) Blath et al.

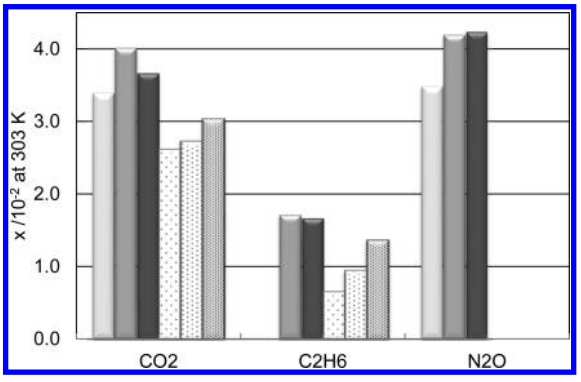

Figure 3. Mole fraction solubility of carbon dioxide, ethane, and nitrous oxide in the ionic liquids studied herein, [$C_n$mim][eFAP], at 303 K. Also represented are the solubilities of the same gases in ionic liquids including the NTf_2^- anion, [$C_n$mim][NTf_2], also at 303 K: light gray, [C_2mim][eFAP]; dark gray, [C_4mim][eFAP]; black, [C_6mim][eFAP]; and dotted, [C_2mim][NTf_2]; 2× dotted, [C_4mim][NTf_2]; 4× dotted, [C_6mim][NTf_2].

to the activation parameter were evaluated by a free-energy perturbation expression in the NpT ensemble using a three-point formula with increments of 2 × 10^{-3} in the activation parameter. We have selected the temperature of 373 K to avoid sampling problems related to the slow dynamics of the ionic liquids.[29]

dx.doi.org/10.1021/jp304501p | J. Phys. Chem. B 2012, 116, 7728−7738

RESULTS AND DISCUSSION

The experimental values obtained for the density of [C_2mim][eFAP], [C_4mim][eFAP], and [C_6mim][eFAP] as a function of pressure and at temperatures from 293 to 353 K are reported in Table 1. The values of density at atmospheric pressure (necessary for the calculation of the gas solubility) were adjusted to linear functions of temperature:

$$\rho_{[C_2mim][eFAP]}/kgm^{-3} = 2060.0 - 1.1897 \times (T/K) \quad (3)$$

$$\rho_{[C_4mim][eFAP]}/kgm^{-3} = 1955.4 - 1.1140 \times (T/K) \quad (4)$$

$$\rho_{[C_6mim][eFAP]}/kgm^{-3} = 1869.5 - 1.0720 \times (T/K) \quad (5)$$

The standard deviation of the fits is always better than 0.1%.

The values determined for [C_2mim][eFAP] and [C_4mim][eFAP] are 0.2% and 0.1% higher than those claimed by the manufacturer at 293 K, respectively. For [C_6mim][eFAP], our values are 0.3% lower than those of Ignat'ev et al.[5] at 293 K and 0.1% lower than those reported by Yao et al.[30] at the same temperature. The values published by Yokozeki et al.[7] at 298 K are 1.4% above those measured herein.

The densities as a function of pressure were correlated using the Tait equation:

$$\rho(T,p) = \left[\frac{\rho^0(T,p^0)}{1 - C\ln\left(\frac{B(T)+p}{B(T)+p^0}\right)}\right] \quad (6)$$

where $\rho^0(T,p^0)$ is the density value at a reference temperature T and at the pressure p^0 = 0.1 MPa; C is an adjustable parameter, and $B(T)$ a polynomial defined by

$$B(T) = \sum_{i=0}^{2} B_i(T)^i \quad (7)$$

The parameters found for the present data are listed in Table 2.

The dynamic viscosity was measured for the three ionic liquids, previously dried, and are listed in Table 3 as a function of temperature from 293 to 373 K. The Vogel−Fulcher−Tammann (VFT) equation was used to correlate the experimental viscosities as a function of temperature of [C_2mim][eFAP], [C_4mim][eFAP], and [C_6mim][eFAP] with a standard deviation of 0.2, 1.0, and 0.3%, respectively:

$$\eta_{[C_2mim][eFAP]}/mPas = (6.90 \times 10^{-3}) \times (T/K)^{1/2} \exp\left[\frac{865}{(T/K) - 159}\right] \quad (8)$$

$$\eta_{[C_4mim][eFAP]}/mPas = (0.60 \times 10^{-3}) \times (T/K)^{1/2} \exp\left[\frac{1214}{(T/K) - 139}\right] \quad (9)$$

$$\eta_{[C_6mim][eFAP]}/mPas = (4.40 \times 10^{-3}) \times (T/K)^{1/2} \exp\left[\frac{949}{(T/K) - 164}\right] \quad (10)$$

The values measured in this work for [C_6mim][eFAP] agree, to within the experimental error, with those reported by Yao et al.[30] at 293 K. The viscosities measured for the three ionic liquids are only slightly higher than those reported for ionic liquids based on the [NTf_2] anion and much lower than those based on the hexafluorophosphate or octylsulfate anions.

Table 9. Thermodynamic Properties of Solvation of Carbon Dioxide, Nitrous Oxide, Ethane, and Nitrogen in the Ionic Liquids [$C_n$mim][eFAP], n = 2,4,6, in the Temperature Range Studied

ionic liquid	$-\Delta_{solv}H^\infty$/kJ mol^{-1}	$-\Delta_{solv}S^\infty$/J mol^{-1} K^{-1}
	CO_2	
[C_2mim][eFAP]	14 ± 2	75 ± 2
[C_4mim][eFAP]	12.5 ± 0.1	68.0 ± 0.5
[C_6mim][eFAP]	12.7 ± 0.2	69 ± 1
	N_2O	
[C_2mim][eFAP]	14 ± 2	75 ± 5
[C_4mim][eFAP]	11 ± 4	63 ± 9
[C_6mim][eFAP]	14 ± 1	72 ± 3
	C_2H_6	
[C_4mim][eFAP]	10 ± 1	68 ± 2
[C_6mim][eFAP]	12 ± 3	73 ± 8
	N_2	
[C_4mim][eFAP]	4 ± 1	58 ± 4

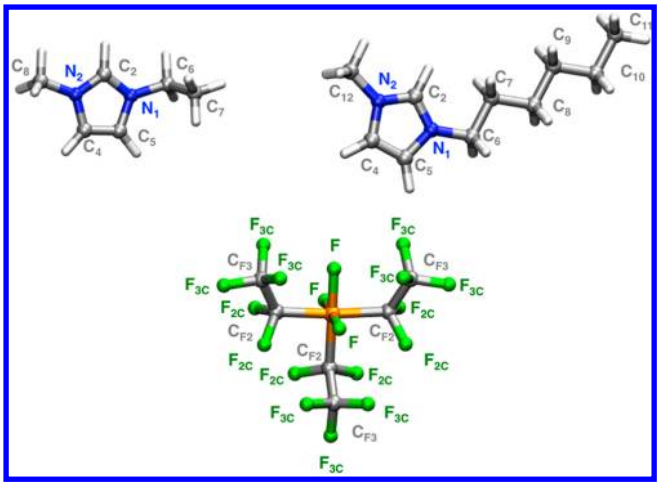

Figure 4. Nomenclature for the sites of the ionic liquids 1-ethyl-3-methyimidazolium tris(pentafluoroethyl)trifluorophosphate and 1-hexyl-3-methylimidazolium tris(pentafluoroethyl)trifluorophosphate used in molecular simulation.

As expected, the viscosity of the [$C_n$mim][eFAP] ionic liquids depend on the length of the alkyl side chain. The viscosities, at 293.15 K, of [C_6mim][eFAP] (118.8 mPa s) and [C_4mim][eFAP] (100.3 mPa s) are 59% and 34% higher than that of [C_2mim][eFAP], respectively. These differences decrease with temperature and are equal to 6% and 1% at 373.15 K, respectively.

In order to determine the miscibility gap in the water + ionic liquid mixtures, the vapor pressure was measured for [C_4mim][eFAP] + water at 303.10 K and for [C_6mim][eFAP] + water at 303.40 and 313.10 K. The results obtained are presented in Table 4 and depicted in Figure 1. Phase separation is determined from the discontinuity of the pressure curves as a function of the composition and, in the present case, phase separation occurs at x_{H_2O} = 0.20 ± 0.03 for [C_4mim][eFAP] at 303.10 K, at x_{H_2O} = 0.43 ± 0.05 for [C_6mim][eFAP] at 303.40 K, and at x_{H_2O} = 0.49 ± 0.07 for [C_6mim][eFAP] at 315.10 K. The water solubility in the ionic liquids increases for larger alkyl side chains of the cation and also increases with temperature. The solubility of the ionic liquid in water appears as negligible as the values of the pressure measured above the biphasic mixtures are very close to those of pure water at the same temperature.

dx.doi.org/10.1021/jp304501p | J. Phys. Chem. B 2012, 116, 7728−7738

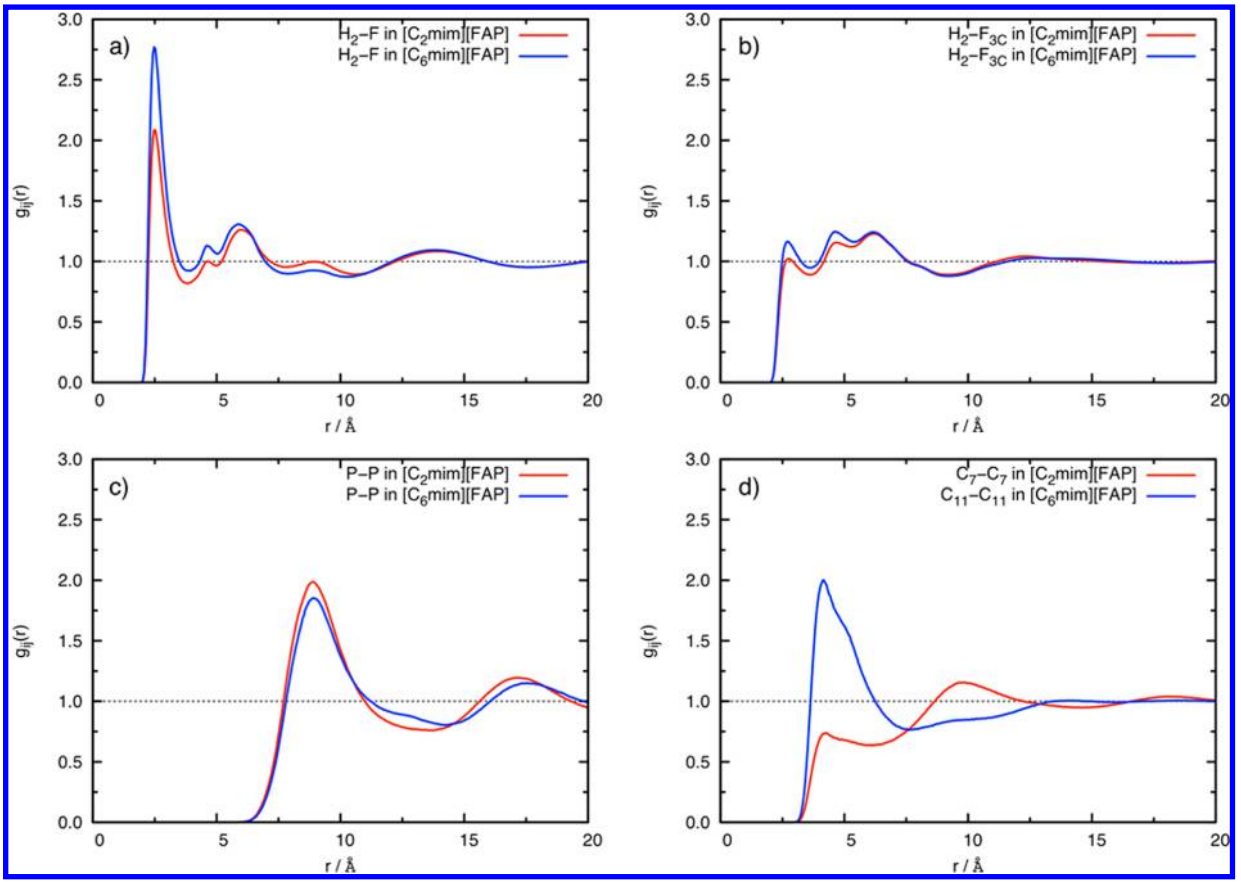

Figure 5. Selected cation−anion site−site RDFs.

For each (gas + ionic liquid) system studied, multiple experimental data points were obtained in the temperature interval between 303 and 343 K in steps of approximately 10 K. The experimental mole fraction solubilities of CO_2 and N_2O in $[C_2mim][eFAP]$, of CO_2, C_2H_6, N_2O, and N_2 in $[C_4mim][eFAP]$ and of CO_2, C_2H_6, and N_2O in $[C_6mim][eFAP]$ are reported in Tables 5−7, respectively. Henry's law constants can be calculated from the experimental values and are used to determine the mole fraction solubility assuming a partial pressure of the gaseous solute equal to 0.1 MPa. The second virial coefficients for the gases, necessary for the calculation of the compressibility factor, were taken from the compilation by Dymond and Smith.[31]

The Henry's law constants have been adjusted to an empirical equation of the form

$$\ln[K_H/10^5\ \text{Pa}] = \sum_{i=0}^{n} A_i (T/K)^{-i} \qquad (11)$$

The coefficients A_i as well as the standard deviations of the fits, considered as a measure of the precision of the experimental solubility data for the different gases in the three ionic liquids are listed in Table 8. The Henry's law constants, calculated from the solubility measurements, are in general considered to be precise to within less than 1%. In the present work, the data for nitrous oxide and nitrogen in $[C_4mim][eFAP]$ seem less precise with a standard deviation of fit around 2%. In order to estimate the accuracy of the solubilities reported, we have represented in Figure 2, the comparison between the Henry's law constants for carbon dioxide in $[C_6mim][eFAP]$ herein and those obtained by other authors. For the temperature range covered, the Henry's law constants agree to within ±5% with those reported by Muldoon et al.[6] and by Zhang et al.[10] and to within ±10% with those reported by Yokozeki et al.[7] and Blath et al.[8]

In Figure 3 are depicted the values for the solubility of the different gases in the three ionic liquids at 303 K. It is observed that the solubilities of carbon dioxide, ethane, and nitrous oxide are higher in the ionic liquids studied herein, $[C_nmim][eFAP]$, than in similar ionic liquids having the bis(trifluorosulfonyl)-amide anion, $[C_nmim][NTf_2]$. Also, the variation of the solubility of the different gases with the length of the alkyl side-chain in the cation of the ionic liquids is different in the two families. For the $[C_nmim][NTf_2]$ family, the gas solubility increases when the alkyl side chains of the imidazolium cations increase from 2 to 6 carbon atoms. For the $[C_nmim][eFAP]$ ionic liquids, the solubility of the three gases studied increases from $n = 2$ to $n = 4$ but then remains constant (to within the mutual experimental uncertainty) when the alkyl side chain increases from 4 to 6 carbon atoms in the imidazolium cation.

In order to try to elucidate the reasons for the behaviors found for the absorption of the different gases by the ionic liquids, we have calculated their thermodynamic properties of solvation.[32] The average values, calculated for the temperature range covered in this work, are listed in Table 9. Both in the case of carbon dioxide and nitrous oxide, the lower solubilities in the ionic liquid $[C_2mim][eFAP]$ are explained by the more negative entropic contributions to the Gibbs energy of solvation, and no differences in the mechanisms of solvation were found in the case of the two other ionic liquids. For ethane, the situation seems slightly different as the enthalpy of solvation is, as expected, slightly more favorable for $[C_6mim][eFAP]$, but it is

dx.doi.org/10.1021/jp304501p | J. Phys. Chem. B 2012, 116, 7728−7738

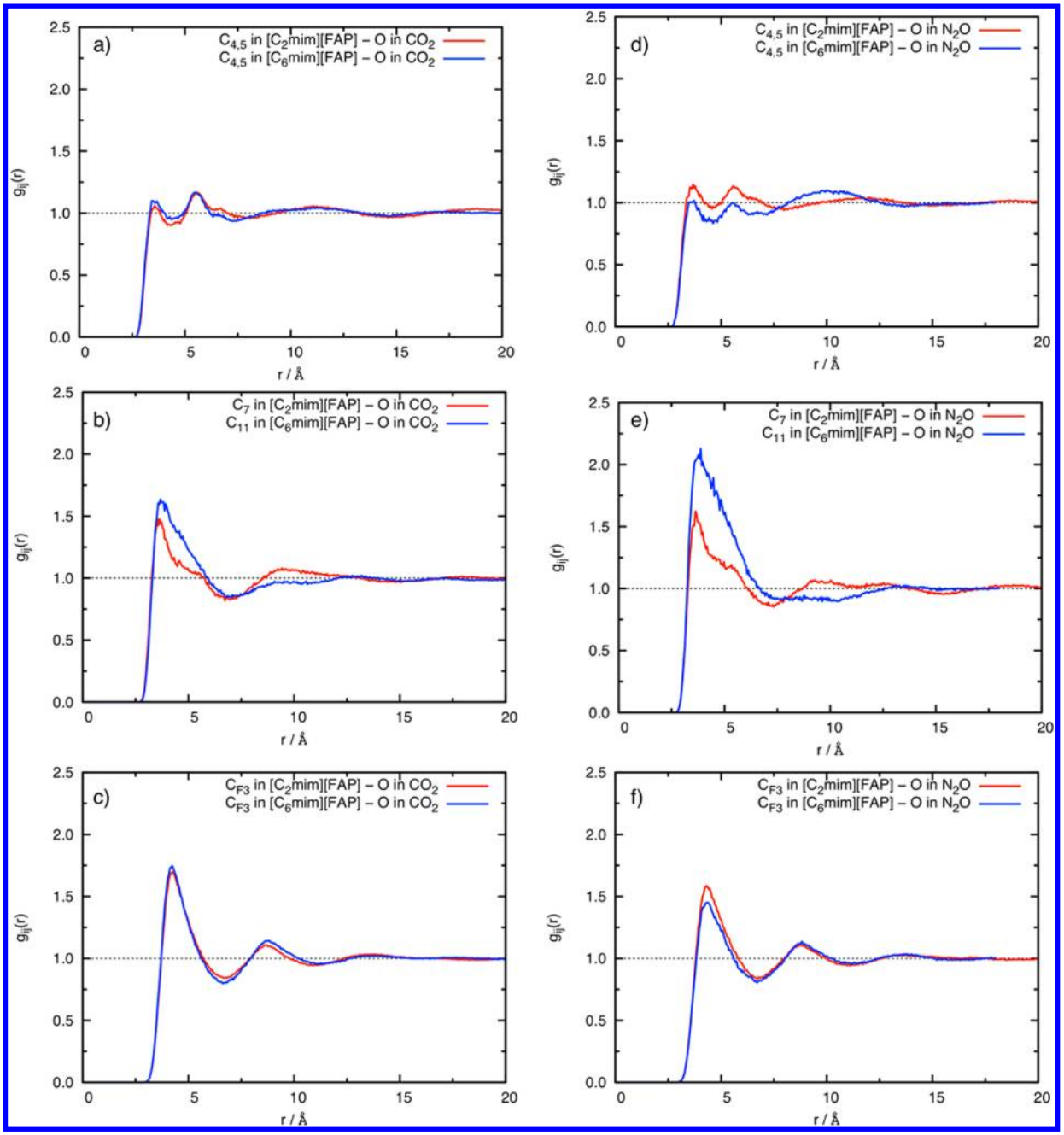

Figure 6. Solute–solvent site–site RDFs of carbon dioxide (left-hand side) and nitrous oxide (right-hand side) in two ionic liquids [C_2mim][eFAP] (in red) and [C_6mim][eFAP] (in blue).

balanced by a more negative entropy of solvation, leading to similar values for the Gibbs energies of solvation.

Molecular simulation was used in order to explain the molecular mechanisms of solvation in these systems. Two gases were chosen, CO_2 and N_2O, in two ionic liquids, [C_2mim][eFAP] and [C_6mim][eFAP]. The nomenclature adopted for the atomic sites of the ionic liquids studied is indicated in Figure 4.

Calculations of the free energy of solvation of CO_2 and N_2O in the ionic liquids [C_2mim][eFAP] and [C_1mim][eFAP] at 373 K allow the calculation of the Henry's law constants, K_H, and of the gas solubility. The calculation of the free energy of solvation of CO_2 in both ionic liquids at 373 K yielded values of $K_H = (132 \pm 13) \times 10^5$ Pa and $K_H = (86.5 \pm 8.6) \times 10^5$ Pa, which correspond to $x_{CO2} = (0.8 \pm 0.1) \times 10^{-2}$ and $x_{CO2} = (1.2 \pm 0.1) \times 10^{-2}$ at a partial pressure $p_{CO2} = 10^5$ Pa for [C_2mim][eFAP] and [C_6mim][eFAP], respectively. Although the calculated solubility values are slightly underestimated, they are sufficiently close to the extrapolated experimental values to validate the force field models used to describe CO_2–ionic liquid interactions.

For N_2O, the values calculated at 373 K are $K_H = (1524 \pm 153) \times 10^5$ Pa and $K_H = (1066 \pm 106) \times 10^5$ Pa, which correspond to $x_{N2O} = (0.7 \pm 0.1) \times 10^{-3}$ and $x_{N2O} = (0.9 \pm 0.1) \times 10^{-3}$ at a partial pressure $p_{N2O} = 10^5$ Pa for [C_2mim][eFAP] and [C_6mim][eFAP], respectively. The values obtained for the gas solubility of N_2O in the two ionic liquids are much lower that the ones obtained experimentally. It is possible that the force field model used to describe the interactions between N_2O and the ionic liquid is not accurate enough. Costa Gomes et al.[25] have observed that, in order to obtain a good agreement between the N_2O solubilities in fluorinated alkanes obtained experimentally

dx.doi.org/10.1021/jp304501p | J. Phys. Chem. B 2012, 116, 7728–7738

and those calculated by molecular simulation, it is necessary to include an unlike interaction parameter, k_{ij} = 0.92, in the Lorentz−Berthelot mixing rules for the Lennard-Jones well-depths $\varepsilon_{ij} = k_{ij}(\varepsilon_{ii}\varepsilon_{jj})^{1/2}$. The parameter k_{ij} could eventually be adjusted to reproduce correctly by molecular simulation the gas solubility values, but a drastic change on the structure of the solutions is not expected.

In Figure 5 are represented the site−site RDFs of representative atoms of the anion and cation of both ionic liquids, showing several features in the liquid-phase structures in the pure ionic liquids. It is observed in panels a and b of Figure 5 that the fluorine atoms of the [eFAP] anion are more probably found close to the hydrogen atom in position C_2 of the imidazolium ring. A more intense peak is observed in the ionic liquid [C_6mim][eFAP], reflecting a stronger structure of this ionic liquid when compared to [C_2mim][eFAP]. This is also reflected, as expected, in the RDFs between the terminal atoms of the alkyl chains of both cations, in agreement with previous experimental[33−35] and molecular simulation[36,37] studies (panel d) of Figure 5). This aspect is no longer present in the [C_2mim][eFAP], the large and voluminous [eFAP]$^-$ anion dominating the structure of the ionic liquid when the side chain of the cation is short.[38] Panel c of Figure 5 shows the RDF between the phosphorus atoms of the anions where a strong peak at a distance around 9 Å can be observed. This peak reflects the strong structure of the anions, an observation compatible with the more important role of larger anions like [eFAP] on the nanoscale organization of the ionic liquid. The different microscopic structures of the liquid phase of these two, relatively similar, ionic liquids can influence the solvation of different species.[11,39,40] One can also expect, as proven before, that even relatively minor differences on the solutes lead to completely different solvation properties, anticipating interesting performances of ionic liquids as reaction or separation media.[41]

Both anions and cations can play an important role on the solubility of different gases on ionic liquids as demonstrated recently by Almantariotis et al.[11] that through partial fluorination of the alkyl chain in an octylimidazolium-based ionic liquid increased the solubility of CO_2 by 20%. We explored the structure of the solutions of CO_2 and N_2O in [C_2mim][eFAP] and [C_6mim][eFAP] in order to gain insights on the molecular mechanisms of solvation in the two gases. Panels a−c of Figure 6 present the RDFs between the oxygen atoms of CO_2 and several representative atoms of the cation and anion of the two ionic liquids. Panels d−f present the RDFs between the oxygen atom of the N_2O molecules and different sites of the ionic liquids.

The RDFs show that CO_2 and N_2O are solvated in similar ways in the ionic liquids [C_2mim][eFAP] and [C_6mim][eFAP], a result compatible with the relatively close experimental solubilities. Both gases interact preferentially with the [eFAP]$^-$ anion, but also with the charged part of the cation. The increase of gas solubility for cations with larger alkyl side-chains is demonstrated by the strong peak observed in panels b and e of Figure 6, more important in the case of [C_6mim][eFAP].

CONCLUSIONS

This work presents an original study of the physicochemical properties of the [$C_n$mim][eFAP] ionic liquids with n = 2, 4, and 6 carbons. Our aim is to study the solvation mechanisms of different gases, relevant for carbon dioxide capture processes, in these ionic liquids with large fluorinated moieties in the anions.

We have observed that the ionic liquids studied are, as expected, more dense than those based on the bis(trifluoromethylsulfonyl) imide anion but present viscosities that are lower which can constitute an advantage for industrial used needing high fluidities.

The [$C_n$mim][eFAP] ionic liquids are only partially miscible with water, the solubility increasing with temperature and with the length of the alkyl side chain in the cation. This result is unexpected as, in other families of ionic liquid, the water immiscibility increases with the increasing length of the alkyl side-chain of the cation. The presence of large fluorinated anions seems to contradict this tendency.

We have also observed that carbon dioxide and nitrous oxide have a high solubility in the [$C_n$mim][eFAP] ionic liquids, its increase not being very significant when the length of the alkyl side-chain of the cation increases. The slightly higher solubility of nitrous oxide can be explained by the more favorable interaction of this gas with the charged part of the ionic liquid, as proven by molecular simulation calculations and by a slightly more negative enthalpy of solvation determined from the experimental data. It is also noteworthy that the solubility of carbon dioxide in [eFAP] based ionic liquids is larger than that in [NTf_2] based ionic liquids with the same cation − at 303.15 K $x_{CO2} = 2.62 \times 10^{-2}$, 2.73×10^{-2} and 3.01×10^{-2} for [C_2mim][NTf_2], [C_4mim][NTf_2], and [C_6mim][NTf_2], respectively; compared with $x_{CO2} = 3.35 \times 10^{-2}$, 3.99×10^{-2} and 3.97×10^{-2} for [C_2mim][eFAP], [C_4mim][eFAP], and [C_6mim][eFAP], respectively. This fact is probably explained by the presence of larger fluorinated moieties in the [$C_n$mim][eFAP] ionic liquids.

Ethane is three times less soluble in the [$C_n$mim][eFAP] ionic liquids and nitrogen is 1 order of magnitude less soluble in the temperature range studied. The solubility of all the gases studied decreases with temperature thus corresponding to exothermic processes of solvation.

AUTHOR INFORMATION

Corresponding Author

*E-mail: margarida.c.gomes@univ-bpclermont.fr.

Notes

The authors declare no competing financial interest.

ACKNOWLEDGMENTS

D.A. thanks the ADEME (Agence de l'Environnement et de la Maîtrise de l'Energie) for financing his Ph.D. O.F. thanks the Université Blaise Pascal for a postdoctoral grant. The FUI ACACIA project is also acknowledged for financing part of this work and the Ph.D. grant of S.S.

REFERENCES

(1) Costa Gomes, M. F.; Husson, P. *ACS Symp. Ser.* **2010**, *1030* (16), 223.
(2) Bates, E. D.; Mayton, R. D.; Ntai, I.; Davis, J. H. J. *J. Am. Chem. Soc.* **2002**, *124*, 926.
(3) Shiflett, M.; Drew, D. W.; Cantini, R. A.; Yokozeki, A. *Energy Fuels* **2010**, *24*, 5781.
(4) Henley, E. J. ; Seader, J. D. ; Roper, D. K. *Separation Process Principles*, 3rd ed.; John Wiley & Sons: New York, 2011.
(5) Ignat'ev, N. V.; Welz-Biermann, U.; Kucheryna, A.; Bissky, G.; Willner, H. *J. Fluorine Chem.* **2005**, *126*, 1150.
(6) Muldoon, M. J.; Aki, S. N. V. K.; Anderson, J. L.; Dixon, J. K.; Brennecke, J. F. *J. Phys. Chem. B* **2007**, *111*, 9001.
(7) Yokozeki, A.; Shiflett, M. B.; Junk, C. P.; Grieco, L. M.; Foo, T. *J. Phys. Chem. B* **2008**, *112*, 16654.
(8) Blath, J.; Christ, J.; Deubler, N.; Hirth, T.; Schiestel, T. *Chem. Eng. J.* **2011**, *172*, 167.

(9) Zhang, X.; Liu, Z.; Wang, W. *AIChE J.* **2008**, *54*, 2717.
(10) Zhang, X.; Huo, F.; Liu, Z.; Wang, W.; Shi, W.; Maginn, E. J. *J. Phys. Chem. B* **2009**, *113*, 7591.
(11) Almantariotis, D.; Gefflaut, T.; Pádua, A. A. H.; Coxam, J.-Y.; Costa Gomes, M. F. *J. Phys. Chem. B* **2010**, *114*, 3608.
(12) Jacquemin, J.; Husson, P.; Padua, A. A. H.; Majer, V. *Green Chem.* **2006**, *8*, 172.
(13) Jacquemin, J.; Husson, P.; Majer, V.; Cibulka, I. *J. Chem. Eng. Data* **2007**, *52*, 2204.
(14) Schilling, G.; Kleinrahm, R.; Wagner, W. *J. Chem. Thermodyn.* **2008**, *40*, 1095.
(15) Jacquemin, J.; Costa Gomes, M. F.; Husson, P.; Majer, V *J. Chem. Thermodyn.* **2006**, *38*, 490.
(16) Jacquemin, J.; Husson, P.; Majer, V.; Costa Gomes, M. F. *Fluid Phase Equilib.* **2006**, *240*, 87.
(17) Husson, P.; Pison, L.; Jacquemin, J.; Costa Gomes, M. F. *Fluid Phase Equilib.* **2010**, *294*, 98.
(18) Canongia Lopes, J. N.; Deschamps, J.; Padua, A. A. H. *J. Phys. Chem. B* **2004**, *108*, 2038.
(19) Canongia Lopes, J. N.; Pádua, A. A. H. *J. Phys. Chem. B* **2004**, *108*, 16893.
(20) Shimizu, K.; Almantariotis, D.; Costa Gomes, M. F.; Pádua, A. A. H.; Canongia Lopes, J. N. *J. Phys. Chem. B* **2010**, *114*, 3592.
(21) Cornell, W. D.; Cieplak, P.; Bayly, C. I.; Gould, I. R.; Merz, K. M.; Fergusin, D. M.; Spellmeyer, D. C.; Fox, T.; Caldwell, J. W.; Kollman, P. A. *J. Am. Chem. Soc.* **1995**, *117*, 5179.
(22) Jorgensen, W. L.; Maxwell, D. S.; Tirado-Rives, J. *J. Am. Chem. Soc.* **1996**, *118*, 11225.
(23) Smith, W.; Forester, T. R. *DL_POLY Molecular Simulation Package*, 2007
(24) Harris, J. G.; Yung, K. H. *J. Phys. Chem.* **1995**, *99*, 12021.
(25) Costa Gomes, M. F.; Deschamps, J.; A.A.H., P. *J. Phys. Chem. B* **2006**, *110*, 18566.
(26) Pensado, A. S.; Costa Gomes, M. F.; Padua, A. A. H. *J. Phys. Chem. B* **2011**, *115*, 3942.
(27) Widom, B. *J. Chem. Phys.* **1963**, *39*, 2808.
(28) Mezei, M. *J. Chem. Phys.* **1987**, *86*, 7084.
(29) Del Pópolo, M. G.; Voth, G. A. *J. Phys. Chem. B* **2004**, *108*, 1744.
(30) Yao, C.; Pitner W., R.; Anderson, L. *J. Anal. Chem.* **2009**, *81*, 5054.
(31) Dymond, J. H.; Smith, E. B. *The Virial Coefficients of Pure Gases and Mixtures*; Clarendon Press: Oxford, 1980.
(32) D. Almantariotis, D.; Fandino, O.; Coxam, J. Y.; Costa Gomes, M. F. *Int. J. Greenhouse Gas Control* **2012**, accepted for publication.
(33) Triolo, A.; Russina, O.; Bleif, H.-J.; Di Cola, E. *J. Phys. Chem. B* **2007**, *111*, 4641.
(34) Triolo, A.; Russina, O.; Fazio, B.; Triolo, R.; Di Cola, E. *Chem. Phys. Lett.* **2008**, *457*, 362.
(35) Russina, O.; Triolo, A.; Gontrani, L.; Caminiti, R.; Xiao, D.; Hines, L. G., Jr; Bartsch, R. A.; Quitevis, E. L.; Plechkova, N.; Seddon, K. R. *J. Phys.: Condens. Matter* **2009**, *21*, 424121.
(36) Wang, Y.; Voth, G. A. *J. Am. Chem. Soc.* **2005**, *127*, 12192.
(37) Canongia Lopes, J. N.; Pádua, A. A. H. *J. Phys. Chem. B* **2006**, *110*, 3330.
(38) Pensado, A. S.; Costa Gomes, M. F.; Canongia Lopes, J. N.; Malfreyt, P.; Padua, A. A. H. *Phys. Chem. Chem. Phys.* **2011**, *13*, 13518.
(39) Jacquemin, J.; Costa Gomes, M .F.; Husson, P.; Majer, V.; Pádua, A. A. H. *Green Chem.* **2008**, *10*, 944.
(40) Costa Gomes, M. F.; Pison, L.; Pensado, A. S.; Padua, A. A. H. *Faraday Disc.* **2012**, *154*, 41.
(41) Pison, L.; Canongia Lopes, J. N.; Rebelo, L. P. N.; Padua, A. A. H.; Costa Gomes, M. F. *J. Phys. Chem. B* **2008**, *112*, 12394.